A reassessment of the sulfur, chlorine and fluorine atmospheric loading during the 1815 Tambora eruption

Manon Pouget, Yves Moussallam, Estelle F. Rose-Koga, Haraldur Sigurdsson

Published in Bulletin of Volcanology – https://doi.org/10.1007/s00445-023-01683-8

A reassessment of the sulfur, chlorine and fluorine atmospheric loading during the 1815 Tambora eruption

Manon Pouget[1@] – Yves Moussallam[2,3] – Estelle F. Rose-Koga[4] – Haraldur Sigurdsson[5]

Corresponding author[@]: manon.pouget21@gmail.com

[1] Université Clermont Auvergne, CNRS, IRD, OPGC, Laboratoire Magmas et Volcans, F-63000 Clermont-Ferrand, France
[2] Lamont-Doherty Earth Observatory, Columbia University, New York NY, 10027, USA
[3] Department of Earth and Planetary Sciences, American Museum of Natural History, New York, NY 10024, USA
[4] Institut Des Sciences de La Terre d'Orléans (ISTO), UO/CNRS, BRGM, 1A Rue de La Férollerie, 45071 Orléans, France
[5] Graduate School of Oceanography, University of Rhode Island, Narragansett, RI 02882, USA

Received: 6 July 2023 / Accepted: 11 October 2023 / Published online: 25 October 2023

Abstract
The 1815 eruption of Mount Tambora (Sumbawa Island, Indonesia), largest known explosive eruption in recorded history, was cataclysmic. It was responsible for a strong short-term global atmospheric cooling the following year, known as "the year without a summer". To evaluate the climatic impact, an accurate quantification of volatile elements degassed during this eruption is crucial. In this study, we re-evaluate the atmospheric release of sulfur, chlorine and fluorine during the 1815 eruption using the petrological approach based on plagioclase-hosted melt inclusions. The pre-eruptive (melt inclusions) and post-eruptive (matrix glass) volatile element concentrations of the magma are measured by electron microprobe. We discuss three different outgassing scenarios and conclude that 147 ± 17 Tg of SO_2, 49 ± 5 Tg of Cl and 20 ± 2 Tg of F were degassed during the eruption, considering closed system ascent and degassing. The SO_2 results take into account the dissolution of sulfides which are present in melt inclusions and plagioclase crystals but not in matrix glasses. Our new estimates are higher than previous estimations from petrological methods or derived from ice cores but are consistent with atmospheric optical depth observations from 1816. The 1815 eruption of Tambora ranks in first place in terms of volcanic SO_2 emission in the last 2000 years, higher than the 1257 Samalas eruption (Lombok Island, Indonesia) if equal methodologies are applied. These estimates remain nonetheless minima as they do not account for the possible additional contribution of a pre-existing gas phase in the magma reservoir.

Keywords Degassing – Volatile elements – Melts inclusions – Petrological method

Introduction

The 1815 eruption of Tambora is known as the largest explosive eruption of the common Era (e.g., Newhall and Self 1982; de Jong Boers 1995). With a Volcanic Explosivity Index (VEI) of 7 (Newhall and Self 1982), the quantity of ash and gases released by the eruption plunged much of Indonesia into darkness for more than three days (de Jong Boers 1995). The plumes formed during the Plinian activity of the eruption carried gases and fine ash well into the stratosphere. Once at stratospheric altitudes, sulfur gases are converted into sulphate aerosols that reflect solar radiation and cause a global cooling of both the troposphere and Earth's surface. In addition, volcanogenic halogens such as chlorine and fluorine have a destructive effect on stratospheric ozone (e.g., Schmidt and Robock 2015). After 1815, both of these effects were observed (e.g., Briffa et al. 1998; D'Arigo et al. 2009). The eruption of Tambora is considered to be the cause of "the year without a summer" in 1816 (e.g., Rampino et al. 1988; Oppenheimer 2003). That year, the surface temperatures were about 0.78 °C colder than average worldwide and the decade 1810–1819 is considered the coldest in more than 500 years (Briffa et al. 1998; D'Arigo et al. 2009). In Europe, summer temperatures were 1–2 °C cooler than average. During the years following 1816 spectacularly colored sunsets and twilights were observed in London, a constant "dry fog" was reported in the northeastern USA and the winters were stormier (e.g., Oppenheimer 2003). Such a global climate perturbation caused crop failure in Indonesia and Europe, thus leading to famines, diseases, and sometimes popular uprising (e.g., de Jong Boers 1995; Oppenheimer 2003). The close relationship between large explosive eruptions and climate has been the subject of many studies including several on Tambora (e.g., de Jong Boers 1995; Devine et al. 1984; Self et al. 2004).

To understand the eruption-climate link it is critical to have a reliable estimate of the bulk amount of sulfur and other volatiles released by the eruption and injected into the stratosphere. The sulfur quantity released by the eruption of Mount Tambora was first estimated at 17 Tg (or 34 Tg SO_2) using melt inclusions contained in plagioclase crystals of

the 1815 magma (Devine et al. 1984). This quantity was later re-estimated at 86 Tg SO_2 and 53–58 Tg SO_2 using the same petrological approach by Sigurdsson and Carey (1992) and Self et al. (2004) respectively. Another method, the study of volcanic sulphate deposits in Antarctic ice cores, gave an estimated output higher than 98 Tg of SO_2 (Legrand and Delmas 1987), later re-evaluated to 45 Tg SO_2 (Sigl et al. 2014).

In this study, we re-evaluate the amounts of volatile elements released during the 1815 Tambora eruption by providing new analyses of S, Cl and F in plagioclase-hosted melt inclusions. We propose three degassing scenarios in order to obtain estimates that are directly comparable with similar studies at other volcanoes.

Volcanological background

Geological setting and past activity

Mount Tambora is a volcano located on Sumbawa Island (Indonesia) which is part of the Sunda Arc (Fig. 1). In this subduction zone, the Indo-Australian plate subducts below the Eurasian plate at a speed of 6–7 cm/y (Hamilton 1979). The Sumbawa sector of this subduction is unique in being composed of young and thin crust which is flanked both to the north and south by oceanic crust (Foden and Varne 1980).

Four older volcanic formations are exposed in the walls of the Tambora caldera, below the 1815 deposits (Sigurdsson and Carey 1992). The oldest one, composed of lava flows, has an age of 43 ka (Barberi et al. 1987). It is overlain by two pyroclastic units and a level of interbedded pyroclastic surge and fall deposits which represents the latest activity of the volcano before the 1815 eruption (Sigurdsson and Carey 1992). From the beginning of its activity, Tambora has produced undersaturated, moderately K_2O-rich magmas ranging from nepheline-normative trachybasalt (Ne-trachybasalt) to Ne-trachyandesite (Foden and Varne 1980).

1815 eruption chronology and stratigraphy

The 1815 eruption of Tambora lasted several days and consisted of two main phases. The first includes four episodes of tephra falls F1, F2, F3 and F4 while the second consists of a succession of pyroclastic flows, surges and co-ignimbrite ash fall (Sigurdsson and Carey 1989).

Phase I: Tephras fall deposits (Fig. 2) (Sigurdsson and Carey 1989)

The first deposit of this sequence is a silt to sand size ash fall layer named F1. This layer is the product of phreatomagmatic activity, and it can be divided into two units suggesting at least two main explosions. It is 1–10 cm thick on the flanks of the volcano and mainly composed of blocky to vesicular pale brown-green pumice, glass shards, dark scoria fragments, crystals of feldspar, biotite, clinopyroxene, magnetite and some lithics. A pale grey-green Plinian pumice fall deposit overlies the F1 unit. This F2 layer was produced by a Plinian eruption which generated a plume 33 km high (Sigurdsson and Carey 1989). It is 10 to 30 cm on the slopes on the volcano. It contains highly vesicular, lapilli sized pale-grey-green pumice and some glass shards. Overlying F2 is a second layer of sandy-silty ash fall, similar to the F1 deposits but more extensive and thicker. This F3 layer is also the product of phreatomagmatic eruptions, and three units can be divided within it, suggesting at least three different explosions. The entire layer is about 10 cm thick close to the edifice and consists of light-colored pumice, glass shards, dark scoria and lithics. This first phase of tephra falls ends with the F4 layer, which is the thickest of the sequence. The F4 layer is the product of another Plinian eruption which generated a plume 43 km high (Sigurdsson and Carey 1989). The deposits are 25 to 30 cm thick on the flanks of Tambora and consists mainly of highly vesicular pale-grey pumice and glass shards. This first phase of phreatomagmatic and Plinian eruptions (F1 to F4) had a duration of more than five days and ejected 4.6 km^3 of tephra (Sigurdsson and Carey 1989).

Phase II: Pyroclastic flows, surges and distal tephra fall (Sigurdsson and Carey 1989)

The second main phase of the 1815 eruption corresponds to the collapse of the second (F4) Plinian volcanic plume, generating pyroclastic surges and flows. The first deposit of this sequence is a pinkish-grey to grey sandy-silty ash surge layer named S1 with pumices and charcoal at some localities. This layer is about 15 cm thick on the volcano's flanks and the pumices reach 2–3 cm in diameter. Overlying S1, is a series of at least 7 pyroclastic flow deposits (PF1, PF2...). They cover almost all of the Sanggar peninsula, reaching the ocean in most directions from the volcano and measure a maximum thickness of 20 m (average about 7 m). Finally, two distal ash falls (F5 and F6) end this second main phase. F5 is 12–25 cm thick and composed of greyish-brown, poorly sorted, silty-sandy ash with some angular pumice clasts. This layer consists of co-ignimbrite ash released by the S1 phase. Unit F6 overlies the S1 unit at some localities with a thickness of 3–4 cm on the western flank of Tambora.

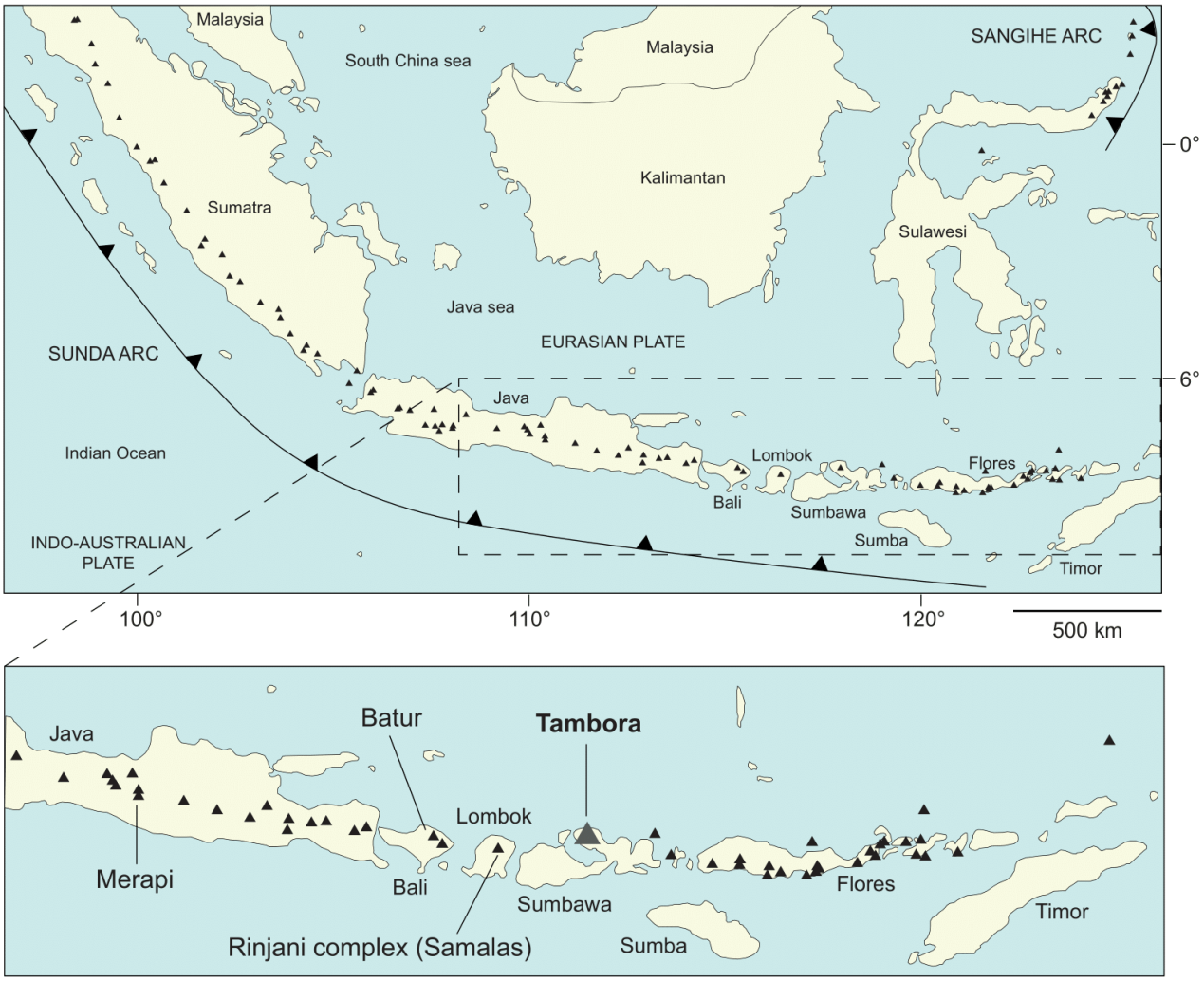

Fig. 1 Map of the Sunda Arc, showing the tectonic setting and the distribution of volcanoes, modified from Gertisser et al. (2012). The enlarged map shows the location of Mount Tambora on Sumbawa island

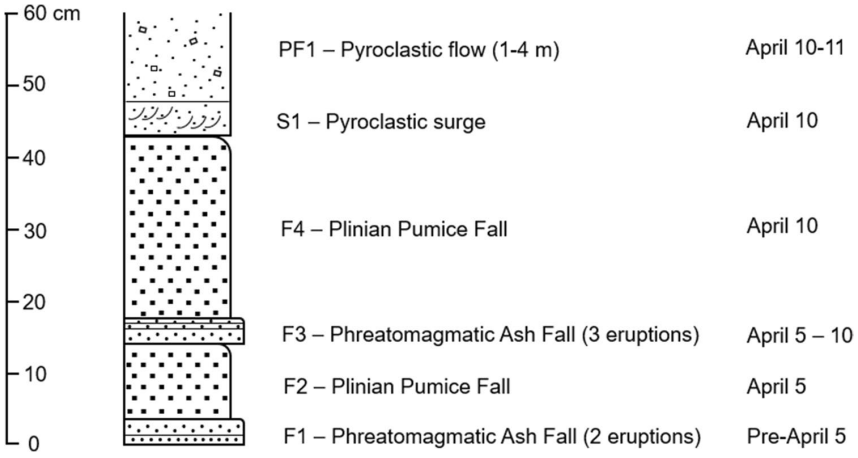

Fig 2 Stratigraphic log of the deposits of the 1815 eruption at 25 km west of the volcano, modified from Sigurdsson and Carey (1989)

Erupted magma volume

The largest uncertainty in estimates of volatile release to the atmosphere during the 1815 eruption is the total erupted magma volume. Based on extensive two-month field work in Sumbawa and on the many smaller nearby islands that surround it, Sigurdsson and Carey (1989) arrived at a total magma volume estimate for the Tambora 1815 eruption of 51 km^3 DRE (dense-rock equivalent). A thorough reevaluation of the erupted volume by Kandlbauer and Sparks (2014), including some new sea floor coring data, and consideration of Tambora's caldera collapse structure, provides a new

revised total volume estimate of 41 ± 4 km^3 DRE. The sulfur, chlorine and fluorine atmospheric loadings calculated from these two estimates are shown in Table S1 in Supplementary Material 1. However, in the remainder of this paper, we report all calculations using the most recent magma volume estimate of 41 km^3 DRE (Kandlbauer and Sparks 2014).

Petrolology and geochemistry of the 1815 magma

Since the beginning of its activity, Tambora has erupted undersaturated potassic magmas, ranging from nepheline-normative trachybasalts to nepheline-normative trachyandesites (Foden and Varne 1980). The 1815 products have a nepheline- trachyandesite composition with high silica content (54–57 wt.% SiO_2), unusual in an island-arc environment (Foden 1986). Pumices are latitic to tephriphonolitic with 30–50% vesicles and contain phenocrysts in a glassy or microcrystal- line matrix. The mineral assemblage is plagioclase > clinopyroxene > magnetite with occasionally small amounts of apatite, biotite and olivine (Gertisser et al. 2012). Foden (1986) found that plagioclase in pumice showed a uniform very calcic population ranging from An_{80} to An_{90}. However, Self et al. (2004) found that the plagioclases can be separated into two distinct populations: (1) unzoned crystals of almost constant composition ($An_{58\pm6}$) and (2) zoned crystals with a very calcic core (≤ An_{91}) and rims with a similar composition as the unzoned ones. Melt inclusions are common in both plagioclase populations. The clinopyroxenes are mostly phenocrysts of Ca-rich augite (Mg_{70}-Mg_{75}) with minor quantities of Ti and Al (Foden 1986; Gertisser et al. 2012).

Sigurdsson and Carey (1989) analysed pumice samples from all the layers of the first main phase and from the seven major pyroclastic flows of the second one. Their bulk rock study showed that “the eruption tapped a very homogenous magma body”. Their range in bulk rock SiO_2 concentrations fell “within the precision of the analytical method” (x-ray fluorescence). The matrix glass analyses confirmed that “the glass composition in falls, surges and flows is identical”. A more recent study (Suhendro et al. 2021) demonstrated a slight evolution in total rock and mineral chemistry between the different eruption phases. Plinian fall units are characterized by a lower phenocryst abundance (avg. of 5.1%) and higher silica content (bulk pumice, 58–58.5 wt.%) than pyro- clastic flow deposits which have a relatively higher crystal abundance (avg. of 12.1%) and a lower silica content (bulk pumice, 56.7–57.9 wt.%; Suhendro et al. 2021). The analysis of the deposit stratigraphy suggests phenocryst stratification in the reservoir was established prior to the 1815 eruption, this being responsible for the slight contrast in bulk compositions (Suhendro et al. 2021).

Materials and methods

In order to quantify S, Cl and F release during the 1815 eruption, we used samples previously collected by Sigurdsson and Carey (1989). The samples used here are tephra from the two Plinian layers of the eruption: sample TB61 from episode F2 and sample TB65 from episode F4 (Fig. 2). This F4 unit can be considered representative of the bulk of the magma, firstly because it was fed by the same ignimbritic magma as unit F5, the most voluminous one (Self et al. 2004) but also because the composition of the melt (matrix glass, melt inclusions) remained identical throughout the entire event (Sigurdsson et al. 1989; Suhendro et al. 2021). For both F2 and F4 samples, tephras are light grey, vesiculated pumices measuring 2 to 3 cm. They have a glassy matrix and contain 10% of phenocrysts which are plagioclase, clinopyroxene and occasionally magnetite, biotite and apatite. We collected plagioclase from these tephra in which melt inclusions are commonly found.

Plagioclase phenocrysts found in tephra can be divided into two subpopulations: crystals with zoned rims and unzoned crystals (Fig. 3). Both populations contain abundant melt inclusions (MI). They range in size from few micrometres to 150 µm in length. We selected MIs that are entirely glassy, oval-shaped and contain a shrinkage bubble (Fig. 4a, c) for analysis; other types (partially crystallized and/or with several bubbles) were excluded (Fig. 4b, c, d).

Sulfide globules have not been reported in previous studies but were found in some of the melt inclusions and plagioclase crystals (Fig. 3). Their size ranges from 1 to 50 µm and they are mostly spherical. No sulfides have been found in the matrix glass.

Analytical methods

Electron microprobe

Major and volatile elements were analysed in selected melt inclusions, matrix glass (MG) and plagioclases by electron microprobe (Cameca SXFive-TACTIS of LMV, Clermont- Ferrand, France) following standard procedure (e.g., Le Voyer 2009; Rose-Koga et al. 2020). Major elements in plagioclase crystals were analysed using a focused beam at 15 nA and 15 kV, whereas melt inclusions and matrix glasses were analysed with a defocused 20 µm beam at 8 nA and 15 kV. For S, Cl, F contents in melt inclusions and matrix glass, a defocused 10 or 20 µm beam at 40 nA and 15 kV was used. Typical errors on measurement for each element are given in 1σ for plagioclase crystals and 3σ for melt inclusions and matrix

glasses: < 1% SiO_2, Al_2O_3, FeO, MgO, CaO, K_2O; <2% Na_2O; <4% TiO_2; <20% MnO, P_2O_5; <10% S, Cl and < 15% F. Procedure characteristics are summarized in Tables S2 and S3 in Supplementary Material 1.

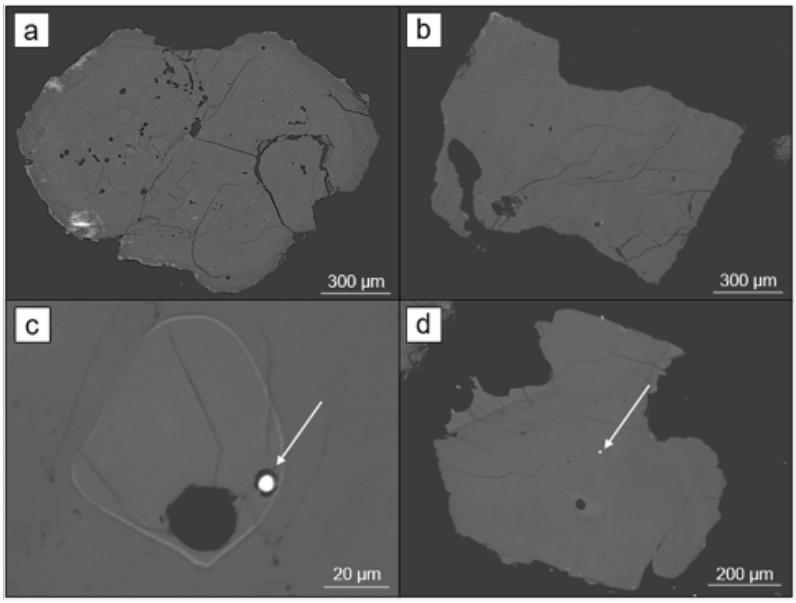

Fig. 3 **a** Plagioclase crystal with zoned rims (TB65_pl15), **b** Unzoned plagioclase crystal (TB65_pl11), **c** Sulfide globule in a plagioclase-hosted melt inclusion (TB65_pl11), **d** Sulfide globule in a plagioclase crystal

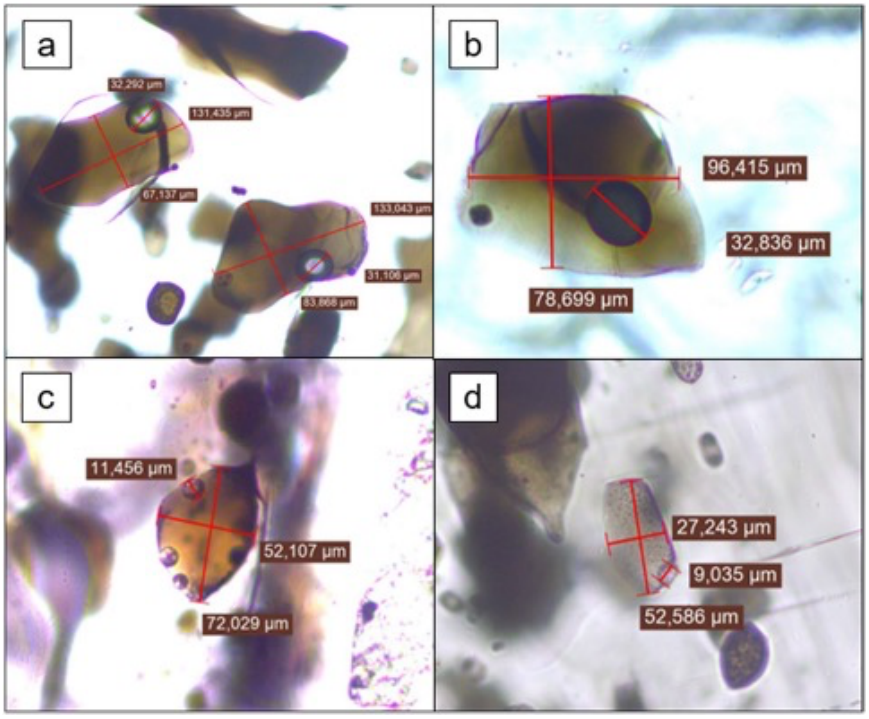

Fig. 4 **a** Glassy, oval-shaped melt inclusions with a shrinkage bubble (TB61_pl19 MI26&27), **b** Melt inclusion containing a sulfide globule (TB61_pl15 MI21), **c** Glassy melt inclusion with several bubbles (TB61_pl5 MI9), **d** Melt inclusion partially crystallized (TB61_pl16 MI10)

Scanning electron microscope (SEM)

After EMPA analysis, a scanning electron microscope (JEOL JSM-5910LV of LMV, Clermont-Ferrand, France) was used to image, in backscattered electrons, the sulfides and plagioclase zoning. Spot analyses were carried out on sulfides with a defocused 56 nm beam at 80 µA and 15 kV.

Petrological method

The petrological method used here was described by Devine et al. (1984), Sigurdsson et al. (1992) and Self et al. (2004) for Tambora and applied to several other eruptions (e.g., Thordarson 2003 for 1783 Laki eruption; Mandeville et al. 1996 for 1883 Krakatau eruption; Vidal et al. 2016 for 1257 Samalas eruption; Peccia et al. 2023 for 43 BCE Okmok eruption). It consists of comparing the pre-eruptive (melt inclusions) and post-eruptive (matrix glass) sulfur, chlorine and fluorine concentrations to estimate by difference the degassed quantities of the respective volatile elements. We used the following mass balance equations to estimate the total masses of SO_2, Cl and F released:

$$E_{SO2} = 2 \times M_v \times (1 - W_{xls}) \times (C_{incl} - C_{matrix}) / 100 \quad (1)$$

$$E_{Cl} = M_v \times (1 - W_{xls}) \times (C_{incl} - C_{matrix}) / 100 \quad (2)$$

$$E_F = M_v \times (1 - W_{xls}) \times (C_{incl} - C_{matrix}) / 100 \quad (3)$$

where E_{SO2} is the SO_2 emission in kg, M_v the mass of erupted magma in kg (1.01×10^{14}), W_{xls} the mass fraction of crystals in the magma (0.115; mean of 0.10 (Self et al. 2004) and 0.13 (Sigurdsson and Carey 1989)) and $C_{incl} - C_{matrix}$ the difference between the average concentrations of the glass inclusion and the matrix glass in wt.%.

We develop three different scenarios in which the C_{incl} value changes. Our goal is to provide estimates that can be directly compared with similar studies that each follow their own set of assumptions. The first scenario uses the volatile concentrations (S, Cl and F) measured in the melt inclusions (MI) that are closest in composition to the bulk rock, considering that it is the most representative of the volatile content of the system prior to eruption. In the second scenario we use the S, Cl and F concentrations of the melt inclusions which have the same FeO content as the matrix glass. This scenario considers that the best estimate of the pre-eruption volatile content is that of the melt at the same level of differentiation as the matrix glass. The third scenario uses the S, Cl and F average concentrations measured in melt inclusions. This scenario considers that variations in MI volatile content can be viewed as statistical distribution centred on a mean or average which best represents the volatile content of the system prior to eruption. This last scenario is mainly used for comparison purpose as it is the method employed by previous studies of the 1815 Tambora eruption.

Results

Chemical composition of plagioclases

Plagioclases from TB61 and TB65 samples showed similar compositions (Table S4 in Supplementary Material 1) falling in the range An_{79}-An_{95} (Fig. 5). This compositional range agrees with the plagioclase cores compositional range of An_{80}-An_{90} reported by Foden (1986), and that of ≤ An_{91} reported by Self et al. (2004) although higher anorthite contents were measured in this study. This range also agrees with the An_{40}-An_{95} range reported by Suhendro et al. (2021).

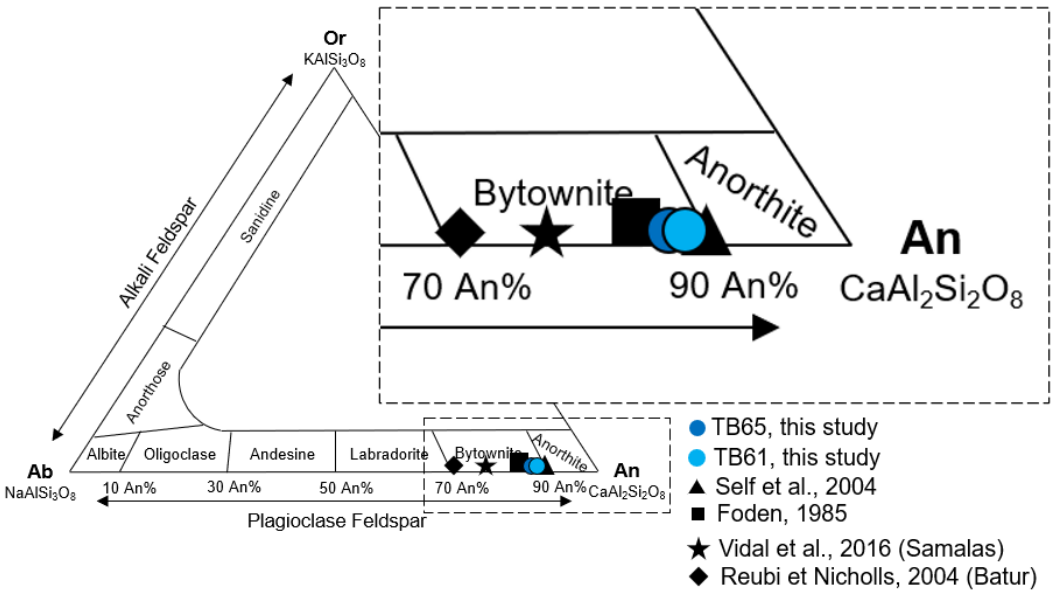

Fig. 5 Feldspar ternary diagram showing the average concentrations of plagioclases in the 1815 tephra from Tambora and data (average) from Samalas and Batur, volcanoes of the same arc

Chemical composition of melt inclusions (MI) and matrix glasses (MG)

Major elements

Major oxides (SiO_2, TiO_2, Al_2O_3, FeO, MnO, MgO, CaO, Na_2O, K_2O, P_2O_5) of 31 melt inclusions and five matrix glasses were analysed by electron microprobe (Table S5 in Supplementary Material 1). Among these 31 inclusions, 11 showed a non-homogeneous texture in SEM, which we interpreted as evidence of post-entrapment crystallization. Only the 20 other, completely glassy melt inclusions are considered in the following. These 20 glassy melt inclusions show homogeneous major element compositions with no significant difference between samples TB61 and TB65 (Table 1). The melt

inclusions contained between 52 and 57 wt.% SiO_2, between 18 and 20 wt.% Al_2O_3 and more than 6 wt.% K_2O. Therefore, they plot in the tephriphonolitic field in a TAS diagram (Na_2O + K_2O vs. SiO_2; Fig. 6). The matrix glasses – being more differentiated and therefore richer in SiO_2 (57–59 wt.%) — lie between phonolite, trachyte and trachyandesite compositions (Fig. 6).

The evolution of silica contents in the melt inclusions and matrix glasses highlights the depletion of iron in the magma during differentiation (Fig. 7). CaO, MgO and TiO_2 also show a restricted < 1 wt.% decrease.

Table 1 Major elements (wt.%) and volatile (ppm) contents of melt inclusions and matrix glasses

	Melt Inclusions						Matrix Glasses					
	TB61 (n=11)		**TB65** (n=9)		**Mean**		**TB61** (n=4)		**TB65** (n=2)		**Mean**	
SiO_2	51.67	(± 0.90)	54.39	(± 0.80)	54.54	(± 0.84)	57.95	(± 0.39)	57.17	(± 0.11)	57.69	(± 0.50)
MgO	1.61	(± 0.22)	1.52	(± 0.15)	1.57	(± 0.19)	1.41	(± 0.02)	1.3	(± 0.01)	1.37	(± 0.06)
FeO	5.11	(± 0.63)	4.82	(± 0.17)	4.98	(± 0.49)	4.49	(± 0.23)	4.47	(± 0.12)	4.48	(± 0.19)
Na_2O	5.21	(± 0.16)	5.28	(± 0.22)	5.24	(± 0.19)	5.41	(± 0.21)	5.52	(± 0.28)	5.45	(± 0.21)
Al_2O_3	18.9	(± 0.39)	19.28	(± 0.25)	19.07	(± 0.38)	19.94	(± 0.24)	19.84	(± 0.07)	19.9	(± 0.19)
K_2O	6.27	(± 0.22)	6.27	(± 0.32)	6.27	(± 0.26)	6.24	(± 0.24)	6.41	(± 0.02)	6.3	(± 0.21)
CaO	3.29	(± 0.38)	3.28	(± 0.51)	3.29	(± 0.43)	3.27	(± 0.11)	3.15	(± 0.03)	3.23	(± 0.10)
TiO_2	0.74	(± 0.13)	0.74	(± 0.05)	0.74	(± 0.10)	0.53	(± 0.03)	0.5	(± 0.02)	0.52	(± 0.03)
P_2O_5	0.56	(± 0.18)	0.61	(± 0.11)	0.58	(± 0.15)	0.37	(± 0.05)	0.46	(± 0.01)	0.4	(± 0.06)
MnO	0.18	(± 0.06)	0.22	(± 0.05)	0.19	(± 0.06)	0.15	(± 0.18)	0.18	(± 0.03)	0.16	(± 0.14)
Total	96.52		96.41		96.47		99.76		99.01		99.51	
S	775	(± 214)	775	(± 142)	775	(± 181)	369	(± 46)	354	(± 16)	364	(± 37)
Cl	1986	(± 229)	2052	(± 213)	2016	(± 219)	1725	(± 101)	1756	(± 35)	1735	(± 81)
F	790	(± 132)	854	(± 196)	819	(± 163)	636	(± 83)	779	(± 90)	683	(± 106)

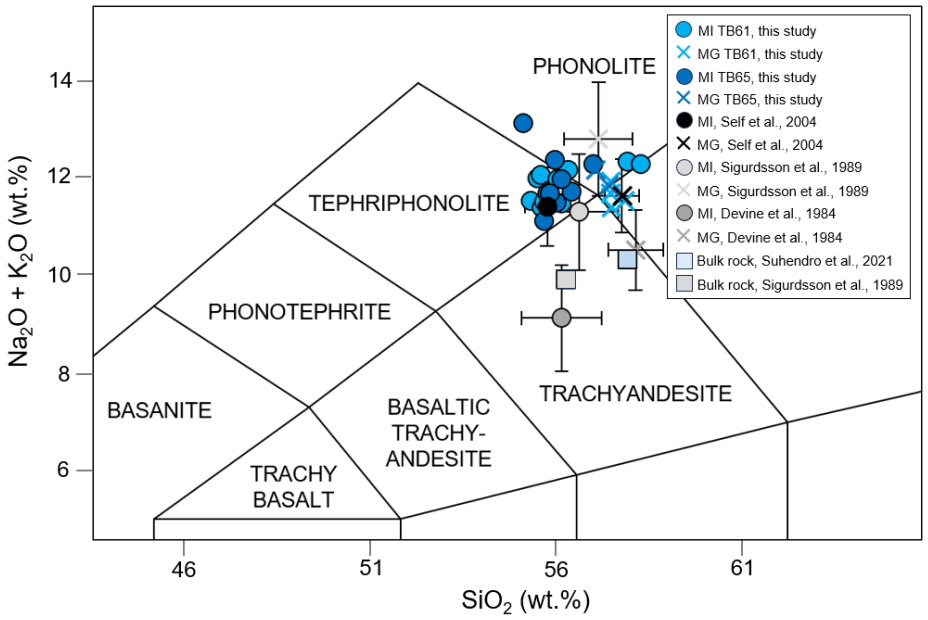

Fig. 6 Total alkali vs silica plot of average alkali concentrations of melt inclusions (MI) and matrix glasses (MG) from four studies (error bars are 1σ standard deviations). All data are normalised to 100%

Volatile elements

When the volatile element content (S, Cl, and F) in the melt inclusions and matrix glasses is greater than 300 ppm, it can be accurately measured by electron microprobe (e.g., Rose-Koga et al. 2020). The analysis of melt inclusions showed sulfur content ranging from 428 ± 28 to 1118 ± 47 ppm S (Fig. 8a), chlorine ranging from 1537 ± 38 to 2253 ± 46 ppm (Fig. 8b) and fluorine ranging from 514 ± 107 to 1253 ± 114 ppm (Fig. 8c). Matrix glasses showed, on average, lower volatile content than melt inclusions (Tables 1 and 2). For sulfur, there was a difference of about 750 ppm between the maximum content in the inclusions and the mean content in the matrix glasses (Table 2). For chlorine, this difference was about 800 ppm. For fluorine the difference was less than 600 ppm (Table 2).

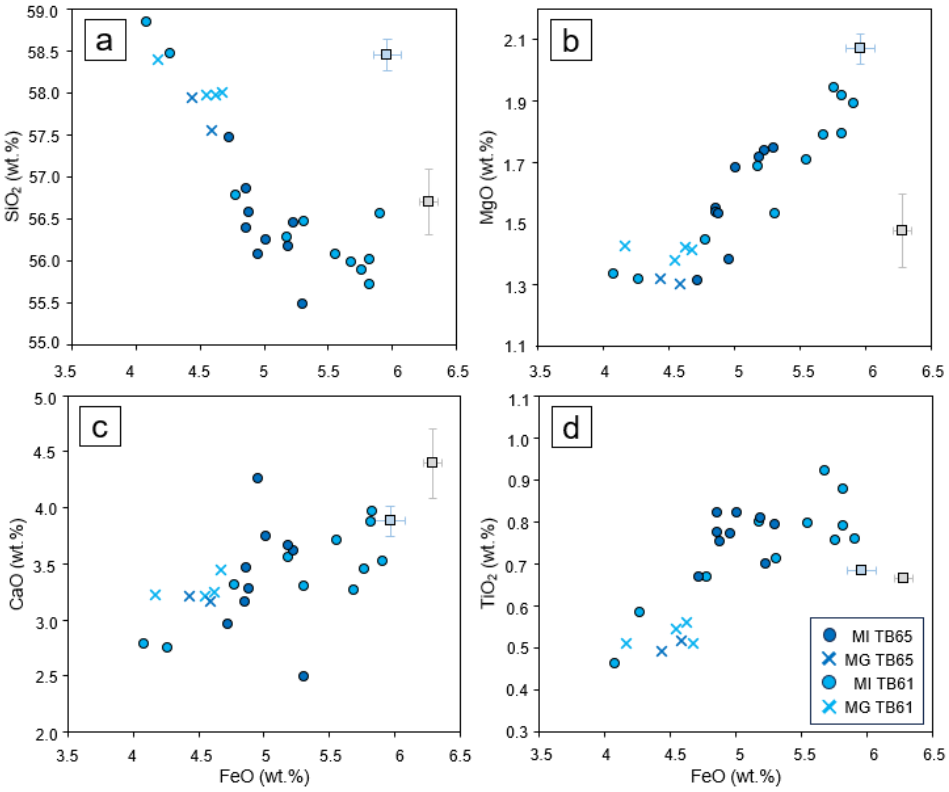

Fig. 7 Trends of major element concentrations in the Tambora magma during its differentiation. All data are normalised. Grey squares are the bulk rock compositions of the F2 and F4 layers from Sigurdsson and Carey (1989). The blue squares are from Suhendro et al. (2021)

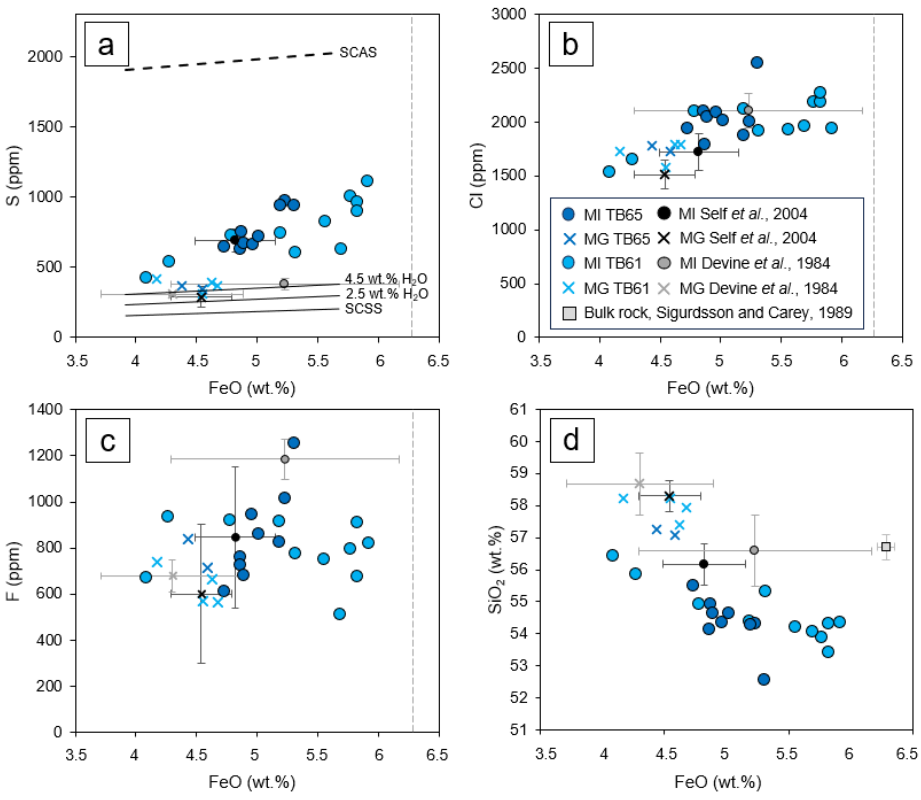

Fig. 8 Trends of volatile element concentrations as a function of FeO (error bars are 1σ standard deviation). The lines are the SCSS (Fortin et al. 2015) with 0, 2.5 and 4.5 wt.% H_2O and the SCAS (Chowdhury and Dasgupta 2019) (1.5 and 3.5 wt.% H_2O are not represented for reasons of clarity). The vertical dotted line is the average FeO content of the bulk rocks of F2 and F4 layers from Sigurdsson and Carey (1989). All data are normalised to 100%

	Melt Inclusions			Matrix Glasses
	Mean	Maximum	At 4.6 wt.% FeO	Mean
S	775 (± 181)	1118	586	364 (± 37)
Cl	2016 (± 219)	2553	1975	1735 (± 81)
F	819 (± 163)	1253	840	683 (± 106)

Table 2 Summary of volatile concentrations (ppm) in melt inclusions and matrix glasses (with 1σ standard deviation)

Sulfides

Sulfide globules (3.6–10.3 ± 0.2 µm) were found in melt inclusions and as inclusions in plagioclase (Fig. 3c, d). The composition of one of these sulfides was measured by SEM and contained 65.7 wt.% Fe, 32.7 wt.% S and 1.7 wt.% Cu (no nickel measurements were made), corresponding to an iron-sulfide composition (pyrrhotite; the copper concentration being too low to be considered a copper-sulfide). Sulfide was neither observed in the matrix glass nor reported in previous studies.

Discussion

Syn-eruptive degassing is widely confirmed both by the few eyewitnesses of the eruption and its gas emissions (e.g., de Jong Boers, 1995). Moreover, climate reports associate the abnormally cold temperatures of 1816 with the presence of a volcanic sulphate aerosol in the atmosphere (Stothers 1984; Rampino et al. 1988; Briffa et al. 1998, D'Arrigo et al. 2009). The melt inclusions richest in S, Cl and F are also the richest in iron and lowest in SiO_2 and are therefore the least evolved (Fig. 8). In contrast, the matrix glasses are the most evolved end-member and have the lowest volatile content (Table 2, Fig. 8). The difference in concentrations, especially of sulfur and chlorine, between the melt inclusions and the matrix glasses gives a first estimate of the total amount of degassed volatiles.

Volatile degassing budget estimates

Estimates of the quantities of SO_2, Cl and F degassed are calculated from mass balance Eqs. (1), (2) and (3). For each volatile element, three degassing scenarios are considered.

The first scenario uses the melt inclusions with compositions closest to that of the F2 and F4 Plinian Fall pumice deposits (Table 3; Sigurdsson and Carey 1989) as starting point. These melt inclusions have some of the highest S, Cl and F concentrations measured (reported in Table 2) suggesting that they represent the original volatile content of the magma before degassing and concomitant crystallisation. In this scenario, it is assumed that the magma rises and degasses in a closed system. It is therefore considered that all the gases exsolved during ascent and crystallization are conserved in the system and participate in the syn-eruptive degassing.

Scenario 2 uses the values of the melt inclusion which have 4.6 wt.% FeO (Table 2). This FeO composition is the one that most closely resembles the composition of the matrix glasses which have an average FeO content of 4.5 wt.% (Table 1). This scenario assumes rising and degassing of the magma in an open system where the exsolved gases can escape before the magma erupts, up until the melt has fully evolved to the composition of the matrix glasses (4.5–4.6 wt.% FeO). Only then does this scenario assumes degassing takes place in a closed system.

Scenario 3 uses the average concentrations of melt inclusions (Table 2). It is not associated with any rising/degassing model but corresponds to the approach of Devine et al. (1984) and Self et al. (2004) and will therefore be used mainly for comparison with literature estimates. The amounts of volatile elements degassed depending on the three scenarios during the eruption are reported in Table 4.

The scenario we judge most appropriate is scenario 1, as it uses melt inclusion compositions most similar to that of the bulk Plinian Fall deposits (Table 3). The assumption we make therefore, is that from this point onward in the melt compositional evolution, all exsolved volatiles remained in the system until the eruption. In this context, we hypothesize a closed-system scenario for magma evolution and ascent, a supposition supported by the exceptional violence of the 1815 Tambora eruption, which achieved a VEI of 7. Scenario 2 by contrast would make the hypothesis of magma evolution and ascent in an open system, a framework more apt for describing volatile emissions from a slow lava flow originating from an open vent volcano. Scenario 1's approach is the same as the one used by Peccia et al. (2023) to estimate the S emission during the 43 BCE eruption of Okmok volcano. Using scenario 1, SO_2 degassing during the 1815 eruption is estimated at 135 ± 14 Tg (68 ± 7 Tg S; Table 4). Also 49 ± 5 Tg of chlorine and 20 ± 2 Tg of fluorine were released (Table 4). These results remain minima for S, as the contribution of sulfides dissolution during the eruption and the possible presence of a deeper gas phase initially present in the magma chamber are not considered in these calculations (Oppenheimer et al. 2011). The pyroclastic flows represent 18 ± 6 km^3 DRE of the total magma volume emitted during the 1815 Tambora eruption (Kandlbauer and Sparks 2014). Pyroclastic flows typically only send gases to the troposphere, although large pyroclastic flow such as in the Okmok II eruption can send gas clouds to the stratosphere (Burgisser et al. 2023; Peccia et al. 2023). Here, if we consider that the PDC only emits sulfur to the troposphere, only 56 % of our estimated SO_2 load might have made it to the stratosphere.

Table 3 Major element composition of the melt inclusions with maximum S and F contents, second highest Cl content (with 1σ standard deviation) and average major element composition of the F2 and F4 bulk rocks from Sigurdsson and Carey (1989) and Suhendro et al. (2021)

	Melt inclusions used for						Bulk rocks			
	S in Scenario 1 (=1118 ppm)		Cl in Scenario 1 (=2282 ppm)		F in Scenario 1 (=908 ppm)		Sigurdsson and Carey (1989)		Suhendro et al. (2021)	
SiO_2	54.36	(±0.18)	54.34	(±0.17)	55.72	(±0.17)	54.57	(±0.39)	58.2	(±0.19)
TiO_2	0.76	(±0.02)	0.79	(±0.02)	0.91	(±0.02)	0.64	(±0.01)	0.68	(±0.01)
Al_2O_3	18.14	(±0.07)	18.73	(±0.07)	19.60	(±0.07)	19.14	(±0.23)	18.57	(±0.06)
FeO	5.68	(±0.15)	5.65	(±0.15)	5.82	(±0.15)	6.05	(±0.07)	5.94	(±0.11)
MnO	0.24	(±0.05)	0.19	(±0.06)	0.08	(±0.06)	0.20	(±0.00)	0.19	(±0.00)
MgO	1.82	(±0.03)	1.74	(±0.02)	1.92	(±0.03)	1.42	(±0.12)	2.06	(±0.05)
CaO	3.38	(±0.04)	3.85	(±0.04)	3.87	(±0.04)	4.23	(±0.31)	3.87	(±0.13)
Na_2O	4.91	(±0.06)	5.06	(±0.06)	5.30	(±0.06)	3.75	(±1.39)	4.46	(±0.07)
K_2O	6.17	(±0.07)	6.04	(±0.07)	6.27	(±0.07)	5.83	(±0.09)	5.85	(±0.10)
P_2O_5	0.64	(±0.03)	0.65	(±0.03)	0.51	(±0.03)	0.42	(±0.02)	0.32	(±0.01)
Total	96.09		97.02		94.75		96.23		100.14	

Table 4 Volatile quantities emitted during the 1815 eruption of Tambra according to the three scenarios (Tg). The total error on the result takes into account the error on the volume on magma emitted, on the fraction of crystals and on the accuracy of the microprobe analyses. The respective errors of each parameter in Eq. (1) were propagated trough the different calculation according to $\sigma_x = \sqrt{\sigma_a^2 + \sigma_b^2}$ if $x = a \pm b$ and to $\frac{\sigma_x}{x} = \sqrt{(\frac{\sigma_a}{a})^2 + (\frac{\sigma_b}{b})^2}$ if $x = a /\times b$

	Scenario 1	Scenario 2	Scenario 3
SO_2	**135±14**	40±4	74±7
Cl	**49±5**	22±2	25±3
F	**20±2**	14±2	12±2

Even without considering sulfide dissolution and a pre-existing gas phase, these new Tambora estimates are higher than those previously estimated by the "classic" petrological method (Table 5). They are two times higher than the estimates of Self et al. (2004) and four times those of Devine et al. (1984). This can mainly be explained by the fact that these authors used the mean values of the melt inclusions in their calculation. Indeed, their results are closer to our scenario 3 (Table 4). In addition, Self et al. (2004) based their calculations on an emitted magma volume of between 30 and 33 km^3 DRE, which is lower than the 41 km^3 DRE used here, hence partially explaining their lower estimations of SO_2 emitted. Devine et al. (1984) and Sigurdsson and Carey (1992) on the other hand, used magma volumes of 87.5 and 51 km^3 DRE respectively. The estimate of Legrand and Delmas (1987) based on ice records (SO_2 > 98 Tg) is closer to our estimates (Table 5) in contrast to the estimate of 45 Tg SO_2 of Sigl et al. (2014), also based on ice core data but using a model calibrated to the quantities of sulfur emitted during the 1991 Pinatubo eruption. Sigl et al. (2014) used the 1991 Pinatubo eruption, for which the quantity of SO_2 degassed had been directly measured by satellite, as a single point reference to establish a function linking the quantity of sulfate aerosols found in ice cores to the quantities emitted during an eruption. The estimate of Legrand and Delmas (1987) by contrast is based on the sulfate aerosol deposition flux per km^2 found in ice cores, which are then converted into a quantity of SO_2 emitted. This discrepancy between estimates derived from ice core data reflects the complexity of volcanic emission reconstruction based on distal sulfate deposits. Our calculated estimate of 135 ± 14 Tg of SO_2 emission aligns remarkably well with the optical depth assessments derived from astronomical observations presented by Stothers (1984). Stothers (1984) estimated a release of 200 Tg of H_2SO_4 into the atmosphere, equivalent to 120 Tg of SO_2, using a compilation of astronomical observations. Their approach encompassed the analysis of cloud shape and colour in locations such as London, New York, and other northern hemisphere regions during the months following the eruption in addition to the observed darkening of the moon during a total lunar eclipse. In contrast to our results, prior estimates of SO_2 release based on petrological analyses by Devine et al. (1984), Sigurdsson et al. (1989), and Self et al. (2004), ranging from 34 to 86 Tg are irreconcilable with the optical depth estimation provided by Stothers (1984).

Method	SO_2 degassed (Tg)	Reference
Petrological	34	Devine et al. 1984
	86	Sigurdsson et al. 1992
	53-58	Self et al. 2004
	147±17	This study
Ice cores	> 98	Legrand et Delmas, 1987
	45	Sigl et al. 2014
Optical depth estimates based on astronomical observations	120	Stothers et al. 1984

Table 5 Estimates of the SO_2 amount degassed during the 1815 eruption of Tambora according to different method and studies

Sulfur degassing and sulfide contribution

Sulfur concentrations measured in lavas or in quench and glassy volcanic products are not necessarily characteristic of their magma source as volatiles degassing and sulfide precipitation or dissolution can occur during ascent and eruption.

The presence of sulfides in melt inclusions and in plagioclase crystals indicates that a fraction of the sulfur originally dissolved in the melt partitioned into these sulfides. It also indicates that the magma was saturated in sulfides during the inclusion-trapping stage and that an equilibrium was established between these sulfides and the magma.

The sulfur concentration at sulfide saturation (SCSS), was calculated using the parameters of Fortin et al. (2015) with a temperature of 950 °C (Self et al. 2004) and a pressure of 0.2 GPa for inclusions (Gertisser et al. 2012) and of 0.1 MPa for matrix glasses (i.e., atmospheric pressure; Fig. 8). The sulfur contents measured in all the melt inclusions are higher than the theoretical SCSS suggesting that the magma was supersaturated in sulfides. This discrepancy could be due to the fact that water is not accounted for in the calculations. However, the SCSS calculated with 1.5, 2.5, 3.5 and 4.5 wt.% H_2O (using the same parameters but only for the MIs) are always lower than the sulfur contents measured in melt inclusions (Fig. 8). Considering more than 4.5 wt.% water in the 1815 magma would not be realistic, with water estimates between 1.5 and 4.5 wt.% H_2O (by difference to 100% in EMPA analyses, this study) or 2–2.5 wt.% H_2O (Sigurdsson et al. 1989). In addition, we tested whether the presence of copper (present in sulfides) and nickel (not measured but potentially present), could play a role in increasing the SCSS. According to tests carried out using the model of Li and Zhang (2022), the addition of copper and/or nickel would decrease the SCSS. Thus, none of the models tested predicts the observed sulfide saturation in the melt inclusions of this study. This could be related to the fact that these models are calibrated mainly on basaltic compositions far from the tephriphonolitic composition of the 1815 magma.

The sulfur concentration at anhydrite saturation (SCAS) line was also calculated (Fig. 8). All our data lies below this line and no sulphate saturation is expected nor observed. This SCAS was calculated according to the parameters of Chowdhury and Dasgupta (2019) and at the same pressures and temperatures as used for the SCSS. The calculations to obtain the SCSS and SCAS lines are presented in Supplementary material 2.

In contrast to the melt inclusions, no sulfides were observed in the matrix glass. This absence indicates that during ascent and eruption, sulfides in matrix glass — that were not trapped in the melt inclusions or in crystals — decomposed, and the lower S concentrations in the matrix imply that this additional S was released to the gas phase and contributed to the degassing. The contribution of sulfides was estimated by calculating the relative volume occupied by sulfide globules in melt inclusions. We assume here that sulfides and inclusions are randomly trapped by growing crystals and that their volumetric proportion is hence representative of the melt at the time of entrapment. We surveyed a total of 62 glassy melt inclusions of which 13 were found to contain sulfides. From 2D images we assumed that sulfides and melt inclusions were spherical in shape to calculate the total volume of each. Using our measured sulfide composition, a sulfide density of 4 g/cm^3 (Robertson et al. 2015) and a total volume of magma emitted of 41 ± 4 km^3 DRE (Kandlbauer and Sparks 2014), we estimated the contribution of sulfide dissolution to a total degassing budget of 12 ± 3 Tg SO_2.

Considering this, the initial estimate of SO_2 degassing of 135 ± 14 Tg in the first scenario, chosen here, now reaches 147 ± 17 Tg. Placed in the context of the last 2000 years of large eruptions worldwide, these new estimates accounting for sulfide dissolution put the 1815 eruption of Tambora in first place in terms of the amount of SO_2 degassed, higher than the 1257 Samalas eruption (Fig. 9). The amount of SO_2 degassed during the latter is re-estimated at 81 ± 3 Tg. This estimate was recalculated based on data from Vidal et al. (2016) and Métrich et al. (2017), following scenario 1 of this study to make it directly comparable. For this, an emitted magma mass of 1.1014 kg (40 km^3 DRE) was considered in mass balance Eqs. (1) and (2), as well as a crystal mass fraction of 0.1 (average value from Métrich et al. 2017). We used the S content reported for the most primitive inclusions from the 1257 Samalas eruption (500 ppm), which most closely match the composition of the bulk deposit, as well as the S content of matrix glasses (50 ppm). The 1815 Tambora eruption and the 1257 Samalas eruption have erupted similar volumes of magma and have the same VEI. However, the melt compositions differ. The 1815 Tambora melt inclusions have a tephriphonolitic composition and record dissolved S up to 1118 ppm while at the 1257 Samalas melt inclusions have a trachydacitic composition and only record up to 500 ppm of dissolved S. It is therefore unsurprising to find that the 1815 Tambora eruption emitted much larger quantities of S to the atmosphere compared to the 1257 Samalas. The same calculation was done for the quantity of chlorine degassed which is estimated at 219 ± 26 Tg.

Halogens degassing and impact on ozone

As chlorine partitions preferentially into the gas phase compared to the melt (e.g., Webster et al. 2009a, 2009b; Beermann et al. 2015), the process of gas exsolution effectively depletes the chlorine content of the melt. This chlorine exsolution process is clearly observed in the magmatic inclusions of the 1815 eruption, which show a difference of about 800 ppm between the most primitive and the most differentiated end members (Fig. 8). For fluorine, whose solubility is less well known, the degassing trend is less obvious except for the TB65 samples which seem to show a strong decrease

in fluorine content in the matrix glasses (Fig. 8). The release of halogens, especially chlorine, into the stratosphere has impacts on its properties and as a result on climate. Once in the stratosphere, halogenated compounds (in the form of HCl, HF or HBr) induce the catalytic destruction of stratospheric ozone (e.g., Textor et al. 2003; Krüger et al. 2015; Schmidt and Robock 2015). This can lead to a partial destruction of the ozone layer which protects the Earth's surface from UV radiation, harmful to many lifeforms. Although there are no data after the 1815 eruption to verify this ozone destruction, Vupputuri (1992) made calculations showing that ozone depletion following the eruption may have been as high as 7% but their calculations did not include chlorine nor fluorine and might hence have been underestimated. The first direct observations of ozone depletion in the stratosphere were made following the eruption of El Chichón in 1882 (DeLuisi et al. 1984). Ozone depletion caused by release of halogens during eruptions is thought to be, in general, more important in subduction zones volcanic systems than in hot spot of rifting zones given their magmas are richer in chlorine (e.g., Scaillet et al. 2003). Some eruptions in arc settings however emit very little to no Cl, with an estimated ≈0 Tg of Cl and F released during the 43 BCE eruption Okmok eruption for instance (Peccia et al. 2023). Our estimated 49 ± 5 Tg Cl and 20 ± 2 Tg F released during the 1815 Tambora eruption appear therefore significant.

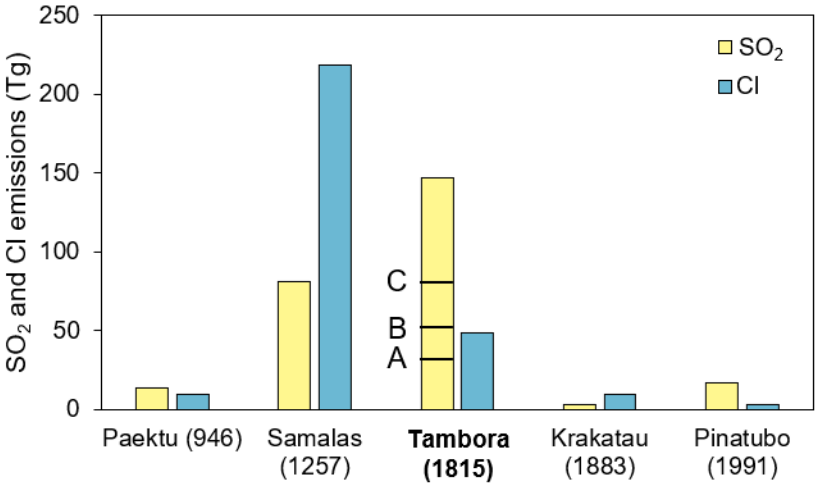

Fig. 9 Quantities of volatiles degassed during the major eruptions of the last two millennia, modified from Vidal et al. (2016). On the Tambora estimates are included the results of previous studies: A Devine et al. (1984), B Self et al. (2004), C Sigurdsson and Carey (1992). The different methods of estimate are given in Table S6 in Supplementary Materials 1

Conclusions

The 1815 Tambora eruption is well known for its global impact on the climate because of the large quantities of volatile elements released to the stratosphere via plumes 33 and 43 km high (Sigurdsson and Carey 1989). In this study, the analysis of melt inclusions and matrix glasses in the products of the Plinian phases (F2 and F4) of the eruption allow us to estimate the amounts of volatile elements (S, Cl and F) degassed during this eruption. Considering degassing and a magma ascent in a closed system, we estimate that 147 ± 17 Tg of SO_2 (74 Tg S) were degassed as well as 49 ± 5 Tg of Cl and 20 ± 2 Tg of F. The SO_2 estimate includes 12 ± 3 Tg coming from the dissolution of sulfides during the eruption. In view of these values, and if comparable methodologies are applied, the 1815 eruption of Tambora appears to be the largest emitter of volcanic SO_2 in the common era. While highly significant, the values obtained in this study could still be considered as minimum values since the contribution of a possible pre-existing exsolved gas phase is not accounted for.

Supplementary information The online version contains supplementary material available at https://doi.org/10.1007/s00445-023-01683-8

Acknowledgements We would like to thank K. Kelley and S. Carey for providing samples. MP thanks G. Georgeais for his help during sample preparation. MP and ER-K greatly appreciated the support and expertise of J-L. Devidal and E. Voyer during EMPA and SEM measurements, respectively. We thank Mike Rampino and an anonymous reviewer for their comments and advice, which helped improve this work. We thank Alexei Ivanov for editorial handling.

Data availability All data obtained in this study are presented in the main text and in the Supplementary Information online.

Declarations

Conflicts of interest The authors declare no conflicts nor competing interest

References

Barberi S, Bigioggero B, Boriani A et al (1987) The Island of Sumbawa; a major structural discontinuity in the Indonesian Arc. Bollettino Della Societa Geologica Italiana 106:547–620

Beermann O, Botcharnikov RE, Nowak M (2015) Partitioning of sulfurand chlorine between aqueous fluid and basaltic melt at 1050°C, 100 and 200MPa. Chem Geol 418:132–157. https://doi.org/10. 1016/j.chemgeo.2015.08.008

Briffa KR, Jones PD, Schweingruber FH, Osborn TJ (1998) Influenceof volcanic eruptions on Northern Hemisphere summer temperature over the past 600 years. Nature 393:450–455. https://doi.org/10.1038/30943

Burgisser A, Peccia A, Plank T, Moussallam Y (2023) Numerical simulations of the latest caldera-forming eruption of Okmok volcano, Alaska. https://doi.org/10.48550/ARXIV.2310.05516

Chowdhury P, Dasgupta R (2019) Effect of sulfate on the basaltic liquidus and Sulfur Concentration at Anhydrite Saturation (SCAS) of hydrous basalts – Implications for sulfur cycle in subduction zones. Chem Geol 522:162–174. https://doi.org/10.1016/j.chemgeo.2019.05.020

D'Arrigo R, Wilson R, Tudhope A (2009) The impact of volcanic forcing on tropical temperatures during the past four centuries. Nature Geosci 2:51–56. https://doi.org/10.1038/ngeo393

de Jong BB (1995) Mount Tambora in 1815: A Volcanic Eruption in Indonesia and Its Aftermath. Indonesia 60:37. https://doi.org/10.2307/3351140

DeLuisi JJ, Mateer CL, Komhyr WD (1984) Effects of the E1 Chichonstratospheric aerosol cloud on Umkehr measurements at Mauna Loa, Hawaii. In: Zerefos CS, Ghaz A (eds) Atmospheric Ozone, D. Reidel, Dordrecht

Devine JD, Sigurdsson H, Davis AN, Self S (1984) Estimates of sulfurand chlorine yield to the atmosphere from volcanic eruptions andpotential climatic effects. J Geophys Res 89:6309–6325. https:// doi.org/10.1029/JB089iB07p06309

Foden J (1986) The petrology of Tambora volcano, Indonesia: A modelfor the 1815 eruption. J Volcanol Geoth Res 27:1–41. https://doi.org/10.1016/0377-0273(86)90079-X

Foden JD, Varne R (1980) The petrology and tectonic setting of Quaternary—Recent volcanic centres of Lombok and Sumbawa, Sunda arc. Chem Geol 30:201–226. https://doi.org/10.1016/0009-2541(80)90106-0

Fortin M-A, Riddle J, Desjardins-Langlais Y, Baker DR (2015) The effect of water on the sulfur concentration at sulfide saturation (SCSS) in natural melts. Geochim Cosmochim Acta 160:100–11.https://doi.org/10.1016/j.gca.2015.03.022

Gertisser R, Self S, Thomas LE et al (2012) Processes and Timescalesof Magma Genesis and Differentiation Leading to the Great Tambora Eruption in 1815. J Petrol 53:271–297. https://doi.org/10. 1093/petrology/egr062

Hamilton WB (1979) Tectonics of the Indonesian Region. USGS Professional Paper 1078, pp 345

Kandlbauer J, Sparks RSJ (2014) New estimates of the 1815 Tambora eruption volume. J Volcanol Geoth Res 286:93–100. https://doi. org/10.1016/j.jvolgeores.2014.08.020

Krüger K, Kutterolf S, Hansteen TH (2015) Halogen release from Plinian eruptions and depletion of stratospheric ozone. In: Schmidt A, Fristad KE, Elkins-Tanton LT (eds) Volcanism and Global Environmental Change, 1st edn. Cambridge University Press, pp 244–259

Le Voyer M (2009) Rôle des fluides dans la genèse des magmas d'arc :analyses in situ des éléments volatils et des isotopes du bore dansles inclusions magmatiques des olivines primitives. Thesis. Université Blaise Pascal - Clermont Ferrand II, France

Legrand M, Delmas RJ (1987) A 220-year continuous record of volcanic H2SO4 in the Antarctic ice sheet. Nature 327:671–676. https://doi.org/10.1038/327671a0

Li H, Zhang L (2022) A thermodynamic model for sulfur content at sulfide saturation (SCSS) in hydrous silicate melts: With implications for arc magma genesis and sulfur recycling. Geochim Cosmochim Acta 325:187–204. https://doi.org/10.1016/j.gca.2022. 03.008

Mandeville CW, Carey S, Sigurdsson H (1996) Magma mixing, fractional crystallization and volatile degassing during the 1883 eruption of Krakatau volcano, Indonesia. J Volcanol Geoth Res 74:243– 274. https://doi.org/10.1016/S0377-0273(96)00060-1

Métrich N, Vidal CM, Komorowski J-C et al (2017) New Insights into Magma Differentiation and Storage in Holocene Crustal Reservoirs of the Lesser Sunda Arc: the Rinjani-Samalas Volcanic Complex (Lombok, Indonesia). J Petrol 58:2257–2284. https:// doi.org/10.1093/petrology/egy006

Newhall CG, Self S (1982) The volcanic explosivity index (VEI) an estimate of explosive magnitude for historical volcanism. J Geophys Res 87:1231. https://doi.org/10.1029/JC087iC02p01231

Oppenheimer C (2003) Climatic, environmental and human consequences of the largest known historic eruption: Tambora volcano (Indonesia) 1815. Prog Phys Geogr: Earth Environ 27:230–259. https://doi.org/10.1191/0309133303pp379ra

Oppenheimer C, Scaillet B, Martin RS (2011) Sulfur Degassing FromVolcanoes: Source Conditions, Surveillance, Plume Chemistry and Earth System Impacts. Rev Mineral Geochem 73:363–421. https://doi.org/10.2138/rmg.2011.73.13

Peccia A, Moussallam Y, Plank T (2023) Melt inclusion and matrix glass data from the 43 BCE eruption of Okmok Volcano. https://doi.org/10.1029/2023GL103334

Rampino MR, Self S, Stothers RB (1988) Volcanic Winters. Annu Rev Earth Planet Sci 16:73–99. https://doi.org/10.1146/annurev.ea.16.050188.000445

Reubi O, Nicholls IA (2004) Magmatic evolution at Batur volcanic field, Bali, Indonesia: petrological evidence for polybaric fractional crystallization and implications for caldera-forming eruptions. J Volcanol Geoth Res 138:345–369. https://doi.org/10.1016/j.jvolgeores.2004.07.009

Robertson JC, Barnes SJ, Le Vaillant M (2015) Dynamics of Magmatic Sulphide Droplets during Transport in Silicate Melts and Implications for Magmatic Sulphide Ore Formation. J Petrology 56:2445–2472. https://doi.org/10.1093/petrology/egv078

Rose-Koga EF, Koga KT, Devidal J-L et al (2020) In-situ measurements of magmatic volatile elements, F, S, and Cl, by electron microprobe, secondary ion mass spectrometry, and heavy ion elastic recoil detection analysis. Am Miner 105:616–626. https://doi.org/10.2138/am-2020-7221

Scaillet B, Luhr JF, Carroll MR (2003) Petrological and volcanologicalconstraints on volcanic sulfur emissions to the atmosphere. In: Robock A, Oppenheimer C (eds) Geophysical Monograph Series.American Geophysical Union, Washington, D. C., pp 11–40

Schmidt A, Robock A (2015) Volcanism, the atmosphere and climatethrough time. In: Schmidt A, Fristad KE, Elkins-Tanton LT (eds) Volcanism and global environmental change, 1st edn. Cambridge University Press, pp 195–207. https://doi.org/10.1017/CBO97 81107415683.017

Self S, Gertisser R, Thordarson T et al (2004) Magma volume, volatileemissions, and stratospheric aerosols from the 1815 eruption of Tambora. Geophys Res Lett 31:L20608. https://doi.org/10.1029/2004GL020925

Sigl M, McConnell JR, Toohey M et al (2014) Insights from Antarcticaon volcanic forcing during the Common Era. Nature Clim Change 4:693–697. https://doi.org/10.1038/nclimate2293

Sigurdsson H, Carey S (1989) Plinian and co-ignimbrite tephra fall from the. Bull Volcanol 51:243–270. https://doi.org/10.1007/BF01073515

Sigurdsson H, Carey S (1992) The Eruption of Tarnbora in 1815: Environmental Effects and Eruption Dynamics. In: Harington IR (ed) The year without a summer? World climate in 1816. Canadian Museum of Nature, Ottawa, pp 16–45

Stothers RB (1984) The Great Tambora Eruption in 1815 and Its Aftermath. Science 224:1191–1198. https://doi.org/10.1126/science.224.4654.1191

Suhendro I, Toramaru A, Miyamoto T et al (2021) Magma chamber stratification of the 1815 Tambora caldera-forming eruption. Bull Volcanol 83:63. https://doi.org/10.1007/s00445-021-01484-x

Textor C, Graf HF, Herzog M, Oberhuber JM (2003) Injection of gasesinto the stratosphere by explosive volcanic eruptions. J Geophys Res 108:4606. https://doi.org/10.1029/2002JD002987

Thordarson T (2003) Atmospheric and environmental effects of the 1783–1784 Laki eruption: A review and reassessment. J Geophys Res 108:4011. https://doi.org/10.1029/2001JD002042

Vidal CM, Métrich N, Komorowski J-C et al (2016) The 1257 Samalaseruption (Lombok, Indonesia): the single greatest stratospheric gas release of the Common Era. Sci Rep 6:34868. https://doi.org/10.1038/srep34868

Vupputuri RKR (1992) The Tambora eruption in 1815 provides a teston possible global climatic and chemical perturbations in the past.Nat Hazards 5:1–16. https://doi.org/10.1007/BF00127136

Webster JD, Sintoni MF, De Vivo B (2009) The partitioning behaviorof Cl, S, and H2O in aqueous vapor- ±saline-liquid saturated phonolitic and trachytic melts at 200 MPa. Chem Geol 263:19–36. https://doi.org/10.1016/j.chemgeo.2008.10.017

Webster JD, Tappen CM, Mandeville CW (2009) Partitioning behavior of chlorine and fluorine in the system apatite–melt–fluid. II: Felsic silicate systems at 200MPa. Geochim Cosmochim Acta 73:559–581. https://doi.org/10.1016/j.gca.2008.10.034